Published in final edited form as:
Nat Genet. 2009 August ; 41(8): 891–898. doi:10.1038/ng.420.

A mouse model of the ATR-Seckel Syndrome reveals that replicative stress during embryogenesis limits mammalian lifespan

Matilde Murga[1], **Samuel Bunting**[2], **Maria F. Montaña**[1], **Rebeca Soria**[1], **Francisca Mulero**[3], **Marta Cañamero**[4], **Youngsoo Lee**[5], **Peter J. McKinnon**[5], **Andre Nussenzweig**[2], and **Oscar Fernandez-Capetillo**[1,*]

[1] Genomic Instability Group; Spanish National Cancer Research Centre (CNIO); Madrid; 28029, Spain.

[2] Experimental Immunology Branch; National Cancer Institute (NIH); Bethesda; MD; 20890; USA

[3] Molecular Imaging Unit; Spanish National Cancer Research Centre (CNIO); Madrid; 28029, Spain.

[4] Comparative Pathology Unit; Spanish National Cancer Research Centre (CNIO); Madrid; 28029, Spain.

[5] Department Genetics and Tumor Cell Biology; St Jude Children's Research Hospital; Memphis; TN 38105, USA.

Abstract

The progressive accumulation of DNA damage is thought to be one of the driving forces that initiates ageing. However, the nature of the damage that arises endogenously is still ill-defined. A known source of endogenous damage is replicative stress (RS), which is intrinsically associated to DNA replication and prevented mainly by the ATR kinase. Here, we have developed a murine model of the human Seckel Syndrome characterized by a severe deficiency in ATR. Seckel mice suffer high levels of RS during embryogenesis when proliferation is widespread, but which decrease to marginal levels in postnatal life. In spite of this decrease, adult Seckel mice present accelerated ageing, which is further aggravated in the absence of p53 due to a further increase of RS. Together, these results support the concept that endogenous RS, particularly *in utero*, contributes to the onset of ageing in postnatal life and this is counterbalanced by the RS-limiting role of the checkpoint proteins ATR and p53.

The accumulation of DNA damage can have important consequences that limit the lifespan of mammalian organisms such as ageing or cancer. On one hand, one of the current theories of ageing is based on the accumulation of DNA damage1. Accordingly, signals of an activated DDR have been shown to increase on aged tissues and stem cells (SC)2،3, and a number of murine models with impaired DNA repair show features of premature ageing4. On the other hand, damaged DNA is the source of the mutations that drive malignant transformation. Therefore, it is not surprising that organisms have evolved complex signalling pathways to protect their DNA. In particular, the so-called DNA damage response (DDR) starts with the

Correspondence should be addressed to O.F. (ofernandez@cnio.es) Phone: +34-91-7328000, Ext: 3480.

Author contributions O.F. designed the study and experiments and wrote the paper. M.M. performed most of the experiments presented. M.F.M. and R.S. helped in the analysis of Seckel MEF and embryos. S.B. and A.N. performed HSC and chromosomal breakage analyses. F.M. helped with the whole body Imaging. M.C. helped with the pathology. Y.L. and P.J.M. performed the analyses of the brains.

The authors declare no competing financial interests.

activation of either one of two members of the PIKK family of protein kinases: Ataxia Telangiectasia Mutated (ATM) and ATM and Rad3-related (ATR)5. Whereas ATM is activated by DNA double strand breaks (DSBs), ATR responds to ssDNA both at resected DSBs as well as at aberrant replicative structures that compromise genome integrity during S phase. Regardless of the kinase that initiates the signalling, the final outcome of the DDR is to promote DNA repair while it delays cell cycle progression until chromosomes are healed.

Whereas ATM deficient animals were generated more than a decade ago[6-8], deciphering the physiological roles of ATR has been hampered by the essential nature of this kinase[9,10]. However, although complete elimination of *Atr* is incompatible with life, a seminal study found a hypomorphic mutation in human patients of a rare human disease known as the Seckel Syndrome (SS) (OMIM 210600)[11]. This disease was first described by Helmut Seckel in 1960 as "bird-headed dwarfism" because of the severe dwarfism and craniofacial features of the patients12. In homozygosity, the mutation brings ATR to almost undetectable levels due to a splicing defect, but yet the protein that is left is sufficient to sustain life. We have here exploited the human *Atr*-Seckel mutation to generate a viable model for the study of ATR function in mammals.

Results

Strategy to develop a murine model of Seckel

One of the mutations that has been genetically linked to the Seckel Syndrome is a synonymous A/G transition in exon 9 (E9) of the *Atr* gene[11]. The mutation promotes the skipping of this exon during the splicing reaction, which results in a severe ATR hypomorphism. We decided to use this information for the generation of a murine model of the human disease. Even though the sequence of E9 and neighbouring exons are very conserved between mouse and human *Atr*, the intronic sequences are highly divergent. We reasoned that since the Seckel mutation affects splicing, the introns and splicing donor/acceptor sequences encompassing *Atr* E9 would likely be necessary to recapitulate the molecular defect. Thus, our strategy was to swap the entire murine genomic fragment encompassing exons 8, 9 and 10 (as well as their internal introns) with the human counterpart and then introduce the Seckel mutation in the E9 of the humanized murine allele ($ATR^{S/S}$, Fig. 1a,b). $ATR^{S/S}$ MEF presented a dramatic splicing deficiency of the humanized transcript at the E8-E10 region; which led to a severe downregulation of ATR protein levels comparable to that observed in cells from ATR-Seckel patients (Fig. 1c-f). Sequencing of the main splicing product of $ATR^{S/S}$ MEF revealed that it corresponded to an aberrant transcript that had skipped E9. Thus, the molecular behaviour of the humanized murine allele developed in this work faithfully recapitulates that of the mutant *Atr* gene previously linked to SS.

Recapitulation of the Seckel Syndrome in $ATR^{S/S}$ mice

$ATR^{S/S}$ mice were born at a sub-mendelian ratio (χ^2, $P<0.0001$; $ATR^{+/+}$[31.8%]| $ATR^{+/S}$[57.8%]|$ATR^{S/S}$[10.4%]) and presented a severe dwarfism which was already noticeable at birth (Fig. 2a-d). Noteworthy, mutant placenta showed an accumulation of necrotic areas and overall loss of cellularity, which could also contribute to the dwarf phenotype regardless of intrinsic developmental defects (Supplementary Fig. 1). In addition to the overall dwarfism, Seckel mice presented a disproportionate decrease in the dimension of their heads, or microcephaly (Fig. 2e and Supplementary Fig. 2). Remarkably, the heads of the mutant mice were not only small but also dysmorphic, presenting several anomalies including the micrognathia and receding forehead characteristic of the human disease (Fig. 2f and Supplementary Fig. 2). While acknowledging the obvious different facial features of mice and humans, the receding forehead phenotype led to the appearance of a protruding nose in

$ATR^{S/S}$ mice, which is reminiscent of the "bird-head" phenotype that originally gave name to the disease (Fig. 2e).

Consistent with the microcephaly, Seckel mice presented a reduction in the size of their brains (Supplementary Fig. 3a). Moreover, Magnetic Resonance Imaging (MRI) analysis revealed profound abnormalities in the brains of $ATR^{S/S}$ mice which included the presence of cysts (6/8 mice analysed) and Agenesis of the Corpus Callosum (AgCC, 8/8 mice) (Fig. 2g). These MRI scans are strikingly similar to those previously obtained from the human SS patients[13]. Consistent with the AgCC observed by MRI, histology revealed a dramatic loss of astrocytes at the corpus callosum of the mutant animals (Supplementary Fig. 3b). Together, these findings suggest that the "bird-head" appearance of Seckel patients derives from a primary developmental defect on the formation of the brain.

Besides the brain; ovaries, testes and all tissues of the haematopoietic compartment of the mutant animals were significantly reduced in size (Supplementary Fig. 4a). Interestingly, whereas at birth ATR levels were reduced in all organs, the difference became postnatally attenuated in some of them such as the testes or lungs (Supplementary Fig. 4b). This might represent a selection for cells in which the percentage of productive splicing was highest among the initial population, and which will particularly occur in tissues with higher replicative indexes. Regardless of its origin, the selective regain of ATR levels suggest an essential role for even minimal amounts of the protein in these organs, as recently described for spermatogenesis in studies performed with a conditional *Atr* allele[14].

The recovery of ATR levels in highly proliferating organs suggests that they could gain a proficient -or at least sufficient- ATR response at adulthood. In agreement with this idea, *in vitro* fertilization could be successfully completed with $ATR^{S/S}$ sperm. In contrast to spermatogenesis, and since all the proliferation linked to oogenesis takes place in the embryo, female gametogenesis would not allow for a postnatal selection of ATR levels and a meiotic defect might persist in the adult. Indeed, no viable oocytes could be obtained even after hormone-induced superovulation of the mutant animals (n=6) and $ATR^{S/S}$ ovaries showed a near complete absence of maturing oocytes (Supplementary Fig. 5a). Whereas the ovaries from newborn $ATR^{S/S}$ animals showed an almost normal density of primordial follicles, a high proportion of these follicles were undergoing degeneration, which is likely indicative of a meiotic recombination defect and would explain the later absence of oocytes in the adult (Supplementary Fig. 5b,c). Importantly, none of the phenotypes found on Seckel mice were detected in a control strain that carried the same humanized allele but without the SS mutation (Fig. 2h,i; Supplementary Fig. 6). Regardless of our novel observations, $ATR^{S/S}$ mice recapitulates all the phenotypic manifestations that are used in the clinic for the diagnosis of SS, including the "bird-headed dwarfism" that originally named the disease.

Development of a progeroid phenotype in Seckel mice

Even though the mutant animals were already smaller at birth, the dwarfism became progressively accentuated in the subsequent months. Ultimately, Seckel mice died with less than half a year presenting a cachexic appearance (Fig. 3a). $ATR^{S/S}$ mice displayed several phenotypes associated with ageing which included hair graying, kyphosis, osteoporosis, accumulation of fat in the bone marrow (BM), decreased density of hair follicles and thinner epidermis (Fig. 3be and data not shown). Analysis of peripheral blood revealed pancytopenia, with decreased numbers of red, white or platelet cells, as it has been reported in Seckel patients (Fig. 3f)[15]. Altogether, these phenotypes indicate the development of a progeroid syndrome in Seckel mice.

To evaluate whether the ageing phenotype was linked to a dysfunction of Stem Cell (SC) compartments, and due to the presence of pancytopenia, we centred our analyses in the

hematopoietic SC (HSC) compartment; one of which is best understood and which dynamics have been analyzed in its relationship to ageing[16]. As mentioned, a first indication of a dysfunctional HSC compartment was the general decrease in cellularity and accumulation of adipose tissue of the $ATR^{S/S}$ BM, which is also observed during normal ageing[17]. Consistently, the analysis of the HSC compartment of the Seckel animals showed similar features to those previously observed in aged mice or humans (Supplementary Fig. 7a-c). First, the frequency of LSK ($Lin^{-}Sca1^{+}Kit^{+}$) cells was reduced in the BM of Seckel animals. Second, the fraction of LT-HSCs was increased and that of the MPPs reduced, within the mutant LSK population[18,19]. In summary, the HSC compartment of young $ATR^{S/S}$ mice resembles that of aged animals.

To determine whether the altered frequency of $ATR^{S/S}$ HSCs was due to cell autonomous effects, we performed mixed BM reconstitution experiments into irradiated wt hosts. Interestingly, and in contrast to other mouse models with deficient DNA repair[3], Seckel BM was found to be equivalent to wt BM in its capacity to reconstitute the granulocyte compartment and was also able to give a significant reconstitution of the lymphocyte compartment (SupplementaryFig. 7d,e). Nonetheless, even though $ATR^{S/S}$ HSCs display a significant repopulating potential when injected into a wt host, the presence of pancytopenia and altered HSC frequencies indicates that non-cell autonomous factors, such as the deterioration of SC niches, must account for their altered function within the mutant mice. As for the HSCs, the overall loss of cellularity, osteoporosis and accumulation of fat on the BM will support this notion. Accordingly, reconstitution of Seckel animals with wt BM does not restore normal thymus size (data not shown). In summary, the presence of pancytopenia in $ATR^{S/S}$ mice derives from altered HSC frequencies that resemble those found in ageing, which likely result from the degeneration of the niche that supports their function.

Besides the generalized age-related decline in organ function, recent works have revealed that human ageing triggers a specific molecular signature, which is characterized by an overall dampening of the IGF-1/GH somatotroph axis[20,21]. Moreover, this response has also been found in murine models of progeria, revealing important molecular similarities between these phenotypes and normal ageing[22,23]. Transcriptional profiling of livers and brains obtained from 3-month old animals revealed such a hallmark on $ATR^{S/S}$ tissues (Supplementary Fig. 8). Interestingly, whereas the dampening of the IGF-1 pathway can also be artificially induced in mice by genotoxic agents22,[23], we failed to find any significant increase in the amount of endogenous DNA damage in these organs in postnatal life (as measured by γH2AX signal or the presence of 53BP1 foci). This is particularly telling in the case of the brain, since given its non-replicative nature ATR should have a limited role in this organ in protecting against postnatal RS. Altogether, our animal, cellular and molecular data demonstrate that the introduction of the Seckel mutation in the mouse leads to the development of a progeroid syndrome that limits the lifespan of the animals.

Seckel as a consequence of an embryonic ATM/DNAPK-dependent DDR

One possibility to reconcile the dampening of IGF-1 on adult tissues in the absence of contemporaneous DNA damage is that this transcriptional programme was initiated in response to an exposure to DNA damage at a previous stage. To determine the cell autonomous effects that could be causative of the phenotype during fetal development, $ATR^{+/+}$ and $ATR^{S/S}$ MEF were analysed. Like human Seckel cells[11], $ATR^{S/S}$ MEF were sensitive to UV or MMS (Supplementary Fig. 9). Nonetheless, even if Seckel MEF were not exposed to exogenous damage, proliferation rates decreased sharply and mutant cells rapidly entered senescence (Fig. 4a). Of note, this happened regardless of whether the cultures were maintained under normoxic conditions. The growth arrest of $ATR^{S/S}$ cells was concomitant with an accumulation of cells at the G2 stage of the cell cycle, which is consistent an activation of the DDR due to replicative

damage (Fig. 4b). In agreement with this, $ATR^{S/S}$ MEF presented a high frequency of cells showing pan-nuclear staining of γH2AX, which is indicative of RS ($ATR^{+/+}$: 0%; $ATR^{S/S}$: 7.6 ±2.3%) (Fig. 4c). In contrast to the γH2AX foci that are present in all cells upon exposure to ionizing radiation, the pan-nuclear staining of γH2AX is equivalent to the one found by inducers of RS such as hydroxyurea (HU), and occurred only in cells which were positive for nuclear cyclin A (Supplementary Fig. 10). Nevertheless, and despite the accumulation of RS, many of the mutant cells also presented 53BP1 foci, which would indicate replication fork collapse and accumulation of DSBs in replicating $ATR^{S/S}$ cells. Accordingly, $ATR^{S/S}$ metaphases presented a high frequency of chromosomal breakage which, consistent with the known role of ATR in maintaining the stability of stalled replication forks[24-26] and suppressing fragile site expression[27,28], frequently occurred at fragile sites (Fig. 4d-f). Thus, Seckel MEF are unable to sustain proliferation *ex vivo* due to the activation of a RS-initiated DDR.

We then investigated which was the kinase responsible for activating the DDR in $ATR^{S/S}$ MEF. Whereas a DNAPKcs inhibitor had no obvious effect, a combined treatment with ATM and DNAPKcs inhibitors virtually eliminated all the γH2AX signal -and 53BP1 foci- in Seckel MEF (Fig. 5a,b). We therefore tested whether the use of the inhibitors could alleviate the growth arrest. However, whereas treatment with the inhibitors alleviated the G2 arrest of the mutant cells (Fig. 5c), this did not translate into a better growth. On the contrary, ATM and DNAPKcs inhibitors were particularly toxic for Seckel MEF (Fig. 5d). Consistent with the synthetic lethal effects observed *in vitro*, ATM deficiency led to embryonic lethality when combined with $ATR^{S/S}$ (data not shown). In summary, the severe downregulation of ATR in MEF leads to the activation of an ATM- and DNAPKcs-dependent DDR in replicating cells due to the accumulation of RS.

Accumulation of RS in Seckel embryos

We finally evaluated whether evidences of RS could also be detected *in vivo*. To this end, γH2AX distribution was analyzed in 13.5 dpc embryos (Supplementary Fig. 11; Fig. 6a). Strikingly, whereas almost no γH2AX is normally detected in wt embryos, $ATR^{S/S}$ littermates showed a dramatic accumulation of cells with pan-nuclear γH2AX throughout the entire embryo. p53 and activated-caspase 3 showed a similar distribution, as proof that many cells were being eliminated by apoptosis at this stage (Fig. 6b,c). Importantly, a similar analysis only revealed a marginal increase of RS or apoptosis in tissues or cells from adult mutant mice such as the brain, colon, BM, proliferating B cells, stomach, liver, lung, kidneys, skin or heart (Fig. 6d and data not shown). The previous result could reflect the high replicative activity of the embryonic stages in contrast to adult tissues. One exception to this occurred on the brain, which undergoes a rapid proliferative burst in the first days of life. In this case, both the embryonic as well as the newborn brain presented apoptosis and RS in the replicating areas (Supplementary Figure 12a-c). In contrast, no proliferation or differentiation defects were observed (Supplementary Fig 12d). It is likely that the particular proliferative expansion of the brain, even within the first days of postnatal life, can contribute to the microcephaly of the mutant animals due to the effects of RS-driven apoptosis. Altogether, our data reveal that Seckel embryos present a generalized activation of the DDR, which is signalled by ATM and DNA-PKcs, and which becomes marginal in postnatal life.

p53 deficiency accelerates ageing initiated by RS

Given that Seckel embryos showed a generalized accumulation of p53, we tested whether p53 deficiency could mitigate some of the ageing phenotypes of the mutant mice. Surprisingly, $ATR^{S/S}/p53^{-/-}$ double mutant animals were born at a very low rate (1.02% from $ATR^{+/S}/p53^{+/-}$ intercrosses, n=294), and the few mice that were born presented a more dramatic progeroid syndrome than their $ATR^{S/S}/p53^{+/+}$ littermates (Supplementary Fig. 13). As a consequence, no $ATR^{S/S}/p53^{-/-}$ mice survived for more than 2 months.

To determine the molecular mechanism by which p53 deficiency exacerbates the Seckel phenotype, $ATR^{+/+}$ and $ATR^{S/S}$ MEF were infected with control and p53 shRNA-expressing retroviruses. Strikingly, whereas the downregulation of p53 in wt MEF slightly increased their growth, it led to a dramatic loss of viability of the mutant cultures accompanied by massive nuclear abnormalities (Fig. 7a,b). One possibility was that the loss of p53 could be driving G2-arrested cells to mitotic catastrophe. On the contrary, p53 depletion in $ATR^{S/S}$ MEF led to a further accumulation of cells in G2 as well as a fourfold increase in the number of cells presenting pan-nuclear γH2AX staining, which indicates that the increased growth rates associated with p53 loss had led to an increase amount of RS on Seckel cells (Fig. 7c,d). In principle, if p53 loss occurs on a background of ATR proficient cells, these cells should still be able to deal with the higher replication rates and to avoid the development of RS. Consistently, whereas $p53^{-/-}$ embryos do not present evidences of RS (Supplementary Fig. 14), $ATR^{S/S}/p53^{-/-}$ embryos showed a dramatic increase of cells with pan-nuclear γH2AX when compared with their $ATR^{S/S}$ littermates (Fig. 7e,f). Moreover, p53 deficiency further increased the number of cells that were eliminated by apoptosis on Seckel embryos, which explains the increased dwarfism of the double mutant animals (Total levels of apoptosis in the embryos: $ATR^{S/S}/p53^{+/+}$: 1.8 ± 0.3%, $ATR^{S/S}/p53^{-/-}$: 6.3% ± 1.1%). In summary, the loss of p53 leads to an increase in the amount of RS suffered by Seckel embryos, which leads to an aggravation of the Seckel phenotypes and further accelerates the onset of ageing on SS mice.

Discussion

$ATR^{S/S}$ as a model for the Seckel Syndrome

The Seckel strain developed in this study recapitulates the human disease to a remarkable extent. In addition to the overall appearance, the previously reported observations including chromosomal instability[15,28-30], progeria or senile appearance[15,31-33] and pancytopenia[15] were all present in Seckel animals. In addition, we also obtained novel data that can help to understand some of the Seckel phenotypes. These included a specific depletion of astrocytes at the corpus callosum as an explanation for the AgCC, the degeneration of the BM and associated HSC dysfunction as the cause of pancytopenia or the placental atrophy and generalized activation of an apoptotic DDR in the embryo as an explanation for the dwarfism. Of particular relevance is the finding that microcephaly could be, at least in part, explained by the exponential replicative expansion that the brain undergoes in the first days of life, which makes it more susceptible to mutations that promote RS.

It is important to note that SS is a variegated disease which has been mapped to 4 different loci, from which only two -*Atr* and *pericentrin*- have been identified[11,34]. Hence, the severity of the phenotypes might differ from case to case. In what regards to the clinical observations made specifically on *Atr*- Seckel patients and, in addition to the phenotypes described above; these patients presented microcrania with fused sutures, dental malocclusion and a deficient closure of the fontalelles[35], all of which were frequent in $ATR^{S/S}$ mice (see Supplementary Fig. 2). Whereas no pancytopenia was reported, the patients were infants at the time of analysis and such a symptom might still develop in the life of the patients. Altogether, we believe the murine model generated in this study constitutes a valid platform for the investigation of the causes, consequences and putative approaches to SS therapy in the laboratory.

Postnatal consequences of an embryonic exposure to DNA damage

In all of the previously published progeroid models the damage particularly accumulated after birth[1,3]. However, whereas we found a generalized activation of the DDR in $ATR^{S/S}$ embryos, we failed to detect a similar increase of endogenous damage on adult tissues. Based on this observation we would want to propose that the accumulation of RS in the embryo has a severe impact on the future onset of ageing and overall well being of adult mice. We here substantiate

our proposal based on a number of arguments. First, organs that are highly proliferative in the adult Seckel mice undergo a selection process so that ATR levels become close to wt. Thus, even if adult $ATR^{S/S}$ animals are ATR proficient in many of their regenerating organs this does not prevent the onset of progeria. This is in agreement with the normal functioning of $ATR^{S/S}$ sperm or HSCs when transplanted into a wt host. Second, the acceleration of the ageing phenotype in p53 deficient $ATR^{S/S}$ mice correlates with a higher accumulation of RS during embryogenesis. Third, adult organs with embryonic RS but no evidence of DNA damage in postnatal life present a transcriptional signature of "aged" organs. Noteworthy, this transcriptional response is activated by the exposure to DNA damage22·23. Finally, even though the elimination of ATR in one-month-old mice leads to the development of a number of progeroid symptoms[14], these mice can survive for up to 19 months (Eric Brown, p. communication). This comparison, by itself, formally proves that embryonic ATR deficiency has a significant impact on future lifespan. One possibility to explain this phenomenon is that the generalized loss of cells by apoptosis during embryogenesis can compromise future stem cell functioning by both limiting SC pools, but particularly because of an alteration of SC niches, as we have seen in the case of HSCs. Taking all together, we propose that the generalized exposure to DNA damage of $ATR^{S/S}$ embryos is responsible for the initiation of a progeroid programme that drives young animals into senescence.

The concept of embryonic dysfunction leading to problems in adulthood has previously been described as "intrauterine programming" (IP)[36-38]. Among other things, IP has been associated to the onset of type-2 diabetes, obsesity, hypertension, cardiac dysfunction, kidney disorders, autoimmunity and osteoporosis. Since the 1920s, a decreased size of the head and brain, accompanied by mental retardation is known to be the main effect of fetal exposure to DNA damage39. Furthermore, intrauterine radiation leads to AgCC in Swiss mice40. Interestingly, the main consequence of the prenatal exposure of rats to RS-inducing agents such as HU was the presence of a number of craniofacial malformations including micrognathia, which is a hallmark of SS[40]. Nevertheless, all of these works evaluated the effects of an acute intrauterine exposure to genotoxic agents so that it is likely that a persistent source of RS, such as in the case of the Seckel embryos, would lead to more prominent and lasting effects. We here would want to add ageing to the list of adult phenotypic manifestations that can arise as a consequence of intrauterine distress.

Ageing by p53 loss

In what relates to ageing, previous genetic experiments in murine models of progeria had invariably shown that the absence of p53 relieves some of the growth disadvantages and, if no cancer arises, enhances the life-span of these animals[41]. Unexpectedly, p53 loss accelerates the ageing of Seckel mice. Besides its effects on ageing, it should be noted that p53 loss also aggravated the "bird-headed dwarfim" phenotypes of the SS animals, this being the first instance in which a connection between p53 loss and microcephalia has been shown. The explanation for this phenomenon seems to lie on the effects of normal levels of p53 on cell cycle progression. Since some of the p53 targets like p21 are well-known inhibitors of CDK activity[42], it is reasonable to think that a modest increase in CDK activity due to p53 loss might enable slightly faster replication kinetics. While ATR-proficient cells may cope with this increase in replication rate, it exacerbates the accumulation of RS when ATR signalling is compromised. Therefore, in the context of the Seckel mutation, the increased amount of damage generated by p53 loss counterbalances the loss of checkpoint function of this TS, further increasing the amount of cells eliminated by apoptosis during embryogenesis. Along these lines, a recent work revealed that loss of Chk1 leads to p53-independent apoptosis in zebrafish, so that a similar pathway might be operating in the $ATR^{S/S}/p53^{-/-}$ animals [43].

Besides its implications for ageing, the synthetic lethal effects of ATR and p53 suggest that fine-tuning of ATR inhibitors could be explored for the selective elimination of p53 deficient tumours. Along these lines, our results can also help to explain the increased sensitivity of p53 deficient tumours to UCN-01, a chemical inhibitor of the ATR target Chk1[44]. Importantly, it is reasonable to think that the synthetic lethal effects of RS with p53 loss could be extensible to other genetic changes that promote faster replication rates, as is the case in many cancer-associated mutations. In this regard, a recent report has shown the counterintuitive finding that p21 loss, in the context of an oncogene that generates DNA damage associated to replication, is tumour suppressive[45]. Thus, in the context of RS, mutations that promote proliferation will boost RS rates even further which, if too high, can limit the viability of the cells. Of note, this is not the first evidence of an ageing suppressive function of the p53 response, since transgenic mice carrying extra alleles of p53 and $p19^{ARF}$ were shown to have an increase in the median life-span[46]. However, our data provide the first genetic evidence showing that p53 loss might promote ageing *in vivo*.

ATR and cancer

Death of Seckel animals was associated with a generalized organic failure, which several organs showing phenotypes that are reminiscent of age-related dysfunction. Nevertheless, in what regards to cancer, and even if ATR has been already shown to be a haploinsufficient tumour suppressor[47], no tumours were ever detected on $ATR^{S/S}$ mice, not even in the absence of p53. One potential explanation is that the toxic effects of the high levels of RS that are linked to severe ATR hypomorphism may counterbalance the increased mutagenicity of Seckel cells. In this manner, whereas a small decrease of ATR might promote cancer, a severe dampening of the ATR response might in contrast be tumour suppressive. Similarly, whereas Chk1 is a haploinsufficient tumour suppressor[48], Chk1 inhibitors are currently being used to kill cancer cells. One striking example of this dichotomy is XPF, where mild mutations are associated with increased cancer susceptibility, whereas mutations that further compromise XPF activity promote progeria[23].

In summary, we have here developed a murine model of the ATR-Seckel syndrome, which faithfully recapitulates the symptoms that have been linked to the human disease and provides a viable model for genetic studies of ATR function in a mammalian organism. Our analysis has revealed that Seckel arises as a consequence of the accumulation of RS during embryonic development, which triggers an ATM-dependent DDR with life-lasting consequences. We believe that incorporating ageing into the battery of phenotypes that can be influenced by fetal distress will help to understand the variability of the ageing process that is observed between individuals.

METHODS

Mice and MEF, and human cells

All animals were kept in a Specific-Pathogen-Free (SPF) barrier zone. Targeting constructs for the generation of humanized $ATR^{S/S}$ and $ATR^{Hs/Hs}$ alleles were generated by recombineering (Genebridges) and used for the generation of heterozygous ES cells. Animals were screened by PCR using the following primers; 3'E8:GGAATAAATCCATGGAAGTGAGAGCAT, 5'N: TCCTCGTCTTTACGGTATCGCC and 5'I7: CACTGGCCTCACAGACTTCAGCATG which yield 500 and 330 bp products for the mutant or wt alleles, respectively. p53 deficient mice have been described before49. MEF were isolated from 12.5 dpc embryos. RT-PCR for splicing at the E8-E10 boundary was performed with primers described before11. Cell cycle was analysed by flow cytometry with propidium iodide. ATM and DNAPKcs inhibitors were kindly provided by Graemme Smith (Astrazeneca, UK) and used at 50 nm and 5 μm,

respectively. Human control and ATR-Seckel fibroblast lines have been described before and were a kind gift of Mark O'Driscoll11.

Metaphase analysis

Analyses of genomic instability were performed on metaphases prepared from MEFs which were treated with 0.1 μg/ml colcemid for one hour. Metaphases were prepared by incubation with 0.1M KCl solution followed by fixation in 3:1 methanol / acetic acid. Telomere repeats were detected by hybridization of a Cy3-conjugated PNA probe. Biotinylated probe for Fra8E1 was prepared by nick translation of a BAC (gift of Thomas Glover). Slides were hybridized overnight, then washed three times in 50% Formamide/2x SSC at 37ºC, three times in 0.1x SSC at 60ºC, and finally in 4x SSC/Tween 20 at 37ºC. Biotinylated probe was detected with streptavidin-Cy5 (Roche). FISH-labeled images were captured using a Zeiss AxioImager M1 epifluorescence microscope (Carl Zeiss MicroImaging Inc, Thornwood, NY) running Metafer (Metasystems Group Inc., Watertown, MA).

p53 downregulation

Control and p53 targeting shRNAs were a kind gift from J. M. Silva (Columbia University, USA). Lentiviral infections were done using standard procedures. To measure the effect of the infection on cell growth and viability, cells were first infected and selected with puromycin. 3 days after selection, an equal number of cells was seeded on a 10 cm dish, and the viability of the cultures was analysed 24 hrs after plating.

Immunofluorescence and immunoblotting

γH2AX (Upstate biotechnology), ATR (Serotec), 53BP1 (Novus Biologicals), p53 (Novocastra) as well as secondary antibodies conjugated with Alexa 488 or Alexa 594 (Molecular probes) were used. Image acquisition was done using a Zeiss Imager Z1 fluorescence microscope with Apotome™ technology. The HT-microscopy mediated analysis of the DDR has been described before[50]. Briefly, cells were grown on μCLEAR bottom 96 well dishes (Greiner Bio-One), and analyzed on a BD Pathway™ 855 BioImager (Beckton Dickinson). Image analysis was performed with the AttoVision software (Beckton Dickinson). All the images for quantitative analyses were acquired under non-saturating exposure conditions. Western analysis were performed on the *LICOR* platform (Biosciences).

IHC

13.5dpc embryos were fixed in formalin and embedded in parafinn for subsequent processing. Consecutive 2.5 μm sections were treated with citrate for antigenic recovery and processed for immunohistochemistry with γH2AX (Upstate), p53 (Novocastra) and activated caspase 3 antibodies. Apoptosis rates were based on the activated caspase 3 signal. Hematoxiline was used to counterstain. Genotyping was performed from a piece of tail. Whole embryo IHCs were scanned with a MIRAX digitalized system (Zeiss) and the digitalized images are available upon request.

Whole body imaging

Whole body imaging was performed on anesthetized animals using the *eXplore Vista* PET-CT (GE Healthcare) and a 7 testla Pharmascan (Bruker). MMWKS software (GE Healthcare) was used for the quantification of the mineral density at the femoral area.

Supplementary Material

Refer to Web version on PubMed Central for supplementary material.

Acknowledgments

We thank Drs. M. Serrano and A. Ramiro for critical comments on the manuscript. We also want to thank Dr. Stephen P. Jackson for his help with the PIKK inhibitors and Aranzazu Garcia for cytometry. M. M. is supported by a Ramón y Cajal contract from the Spanish Ministry of Science (RYC-2003-002731) and from a grant from Fondo de Investigaciones Sanitarias (PI080220). Work in O. F.'s laboratory is supported by grants from the Spanish Ministry of Science (RYC-2003-002731, CSD2007-00017 and SAF2008-01596), EMBO Young Investigator Programme, European Research Council (ERC-210520) and Epigenome Network of Excellence (EU-FP6).

References

1. Lombard DB, et al. DNA repair, genome stability, and aging. Cell 2005;120:497–512. [PubMed: 15734682]
2. Sedelnikova OA, et al. Senescing human cells and ageing mice accumulate DNA lesions with unrepairable double-strand breaks. Nat Cell Biol 2004;6:168–70. [PubMed: 14755273]
3. Rossi DJ, et al. Deficiencies in DNA damage repair limit the function of haematopoietic stem cells with age. Nature 2007;447:725–9. [PubMed: 17554309]
4. Schumacher B, Garinis GA, Hoeijmakers JH. Age to survive: DNA damage and aging. Trends Genet 2008;24:77–85. [PubMed: 18192065]
5. Harper JW, Elledge SJ. The DNA damage response: ten years after. Mol Cell 2007;28:739–45. [PubMed: 18082599]
6. Xu Y, Baltimore D. Dual roles of ATM in the cellular response to radiation and in cell growth control. Genes Dev 1996;10:2401–10. [PubMed: 8843193]
7. Elson A, et al. Pleiotropic defects in ataxia-telangiectasia protein-deficient mice. Proc Natl Acad Sci U S A 1996;93:13084–9. [PubMed: 8917548]
8. Barlow C, et al. Atm-deficient mice: a paradigm of ataxia telangiectasia. Cell 1996;86:159–71. [PubMed: 8689683]
9. Brown EJ, Baltimore D. Essential and dispensable roles of ATR in cell cycle arrest and genome maintenance. Genes Dev 2003;17:615–28. [PubMed: 12629044]
10. de Klein A, et al. Targeted disruption of the cell-cycle checkpoint gene ATR leads to early embryonic lethality in mice. Curr Biol 2000;10:479–82. [PubMed: 10801416]
11. O'Driscoll M, Ruiz-Perez VL, Woods CG, Jeggo PA, Goodship JA. A splicing mutation affecting expression of ataxia-telangiectasia and Rad3-related protein (ATR) results in Seckel syndrome. Nat Genet 2003;33:497–501. [PubMed: 12640452]
12. Seckel, H. Bird-Headed Dwarfs: Studies in Developmental Anthropology Including Human Proportions. Charles C. Thomas; Springfield, IL: 1960.
13. Shanske A, Caride DG, Menasse-Palmer L, Bogdanow A, Marion RW. Central nervous system anomalies in Seckel syndrome: report of a new family and review of the literature. Am J Med Genet 1997;70:155–8. [PubMed: 9128935]
14. Ruzankina Y, et al. Deletion of the developmentally essential gene ATR in adult mice leads to age-related phenotypes and stem cell loss. Cell Stem Cell 2007;1:113–26. [PubMed: 18371340]
15. Butler MG, Hall BD, Maclean RN, Lozzio CB. Do some patients with Seckel syndrome have hematological problems and/or chromosome breakage? Am J Med Genet 1987;27:645–9. [PubMed: 3115102]
16. Rossi DJ, Jamieson CH, Weissman IL. Stems cells and the pathways to aging and cancer. Cell 2008;132:681–96. [PubMed: 18295583]
17. Rosen CJ, Bouxsein ML. Mechanisms of disease: is osteoporosis the obesity of bone? Nat Clin Pract Rheumatol 2006;2:35–43. [PubMed: 16932650]
18. Morrison SJ, Wandycz AM, Akashi K, Globerson A, Weissman IL. The aging of hematopoietic stem cells. Nat Med 1996;2:1011–6. [PubMed: 8782459]
19. Sudo K, Ema H, Morita Y, Nakauchi H. Age-associated characteristics of murine hematopoietic stem cells. J Exp Med 2000;192:1273–80. [PubMed: 11067876]
20. Bartke A. Minireview: role of the growth hormone/insulin-like growth factor system in mammalian aging. Endocrinology 2005;146:3718–23. [PubMed: 15919742]

21. Lombardi G, Di Somma C, Rota F, Colao A. Associated hormonal decline in aging: is there a role for GH therapy in aging men? J Endocrinol Invest 2005;28:99–108. [PubMed: 16042367]
22. van der Pluijm I, et al. Impaired genome maintenance suppresses the growth hormone--insulin-like growth factor 1 axis in mice with Cockayne syndrome. PLoS Biol 2007;5:e2. [PubMed: 17326724]
23. Niedernhofer LJ, et al. A new progeroid syndrome reveals that genotoxic stress suppresses the somatotroph axis. Nature 2006;444:1038–43. [PubMed: 17183314]
24. Cha RS, Kleckner N. ATR homolog Mec1 promotes fork progression, thus averting breaks in replication slow zones. Science 2002;297:602–6. [PubMed: 12142538]
25. Sogo JM, Lopes M, Foiani M. Fork reversal and ssDNA accumulation at stalled replication forks owing to checkpoint defects. Science 2002;297:599–602. [PubMed: 12142537]
26. Stiff T, et al. Nbs1 is required for ATR-dependent phosphorylation events. Embo J 2005;24:199–208. [PubMed: 15616588]
27. Casper AM, Nghiem P, Arlt MF, Glover TW. ATR regulates fragile site stability. Cell 2002;111:779–89. [PubMed: 12526805]
28. Casper AM, Durkin SG, Arlt MF, Glover TW. Chromosomal instability at common fragile sites in Seckel syndrome. Am J Hum Genet 2004;75:654–60. [PubMed: 15309689]
29. Bobabilla-Morales L, et al. Chromosome instability induced in vitro with mitomycin C in five Seckel syndrome patients. Am J Med Genet A 2003;123A:148–52. [PubMed: 14598338]
30. Syrrou M, Georgiou I, Paschopoulos M, Lolis D. Seckel syndrome in a family with three affected children and hematological manifestations associated with chromosome instability. Genet Couns 1995;6:37–41. [PubMed: 7794560]
31. Arnold SR, Spicer D, Kouseff B, Lacson A, Gilbert-Barness E. Seckel-like syndrome in three siblings. Pediatr Dev Pathol 1999;2:180–7. [PubMed: 9949225]
32. Boscherini B, et al. Intrauterine growth retardation. A report of two cases with bird-headed appearance, skeletal changes and peripheral GH resistance. Eur J Pediatr 1981;137:237–42. [PubMed: 7198044]
33. Fathizadeh A, Soltani K, Medenica M, Lorincz AL. Pigmentary changes in Seckel's syndrome. J Am Acad Dermatol 1979;1:52–4. [PubMed: 500866]
34. Griffith E, et al. Mutations in pericentrin cause Seckel syndrome with defective ATR-dependent DNA damage signaling. Nat Genet 2008;40:232–6. [PubMed: 18157127]
35. Goodship J, et al. Autozygosity mapping of a seckel syndrome locus to chromosome 3q22. 1-q24. Am J Hum Genet 2000;67:498–503. [PubMed: 10889046]
36. Fowden AL, Giussani DA, Forhead AJ. Intrauterine programming of physiological systems: causes and consequences. Physiology (Bethesda) 2006;21:29–37. [PubMed: 16443820]
37. Fowden AL, Forhead AJ, Coan PM, Burton GJ. The placenta and intrauterine programming. J Neuroendocrinol 2008;20:439–50. [PubMed: 18266944]
38. Barker D. The fetal origins of adult disease. Proc R Soc Lond B Biol Sci 1995;262:37–43.
39. Murphy DP. Ovarian radiation—its effect on the health of subsequent children. Review of the literature, experimental and clinical, with a report of 320 human pregnancies. Surg Gynecol Obstet 1928:47.
40. Schmidt SL, Lent R. Effects of prenatal irradiation on the development of cerebral cortex and corpus callosum of the mouse. J Comp Neurol 1987;264:193–204. [PubMed: 3680628]
41. Rodier F, Campisi J, Bhaumik D. Two faces of p53: aging and tumor suppression. Nucleic Acids Res 2007;35:7475–84. [PubMed: 17942417]
42. el-Deiry WS, et al. WAF1, a potential mediator of p53 tumor suppression. Cell 1993;75:817–25. [PubMed: 8242752]
43. Sidi S, et al. Chk1 suppresses a caspase-2 apoptotic response to DNA damage that bypasses p53, Bcl-2, and caspase-3. Cell 2008;133:864–77. [PubMed: 18510930]
44. Wang Q, et al. UCN-01: a potent abrogator of G2 checkpoint function in cancer cells with disrupted p53. J Natl Cancer Inst 1996;88:956–65. [PubMed: 8667426]
45. Viale A, et al. Cell-cycle restriction limits DNA damage and maintains self-renewal of leukaemia stem cells. Nature 2009;457:51–6. [PubMed: 19122635]

46. Matheu A, et al. Delayed ageing through damage protection by the Arf/p53 pathway. Nature 2007;448:375–9. [PubMed: 17637672]

47. Brown EJ, Baltimore D. ATR disruption leads to chromosomal fragmentation and early embryonic lethality. Genes Dev 2000;14:397–402. [PubMed: 10691732]

48. Liu Q, et al. Chk1 is an essential kinase that is regulated by Atr and required for the G(2)/M DNA damage checkpoint. Genes Dev 2000;14:1448–59. [PubMed: 10859164]

49. Jacks T, et al. Tumor spectrum analysis in p53-mutant mice. Curr Biol 1994;4:1–7. [PubMed: 7922305]

50. Murga M, et al. Global chromatin compaction limits the strength of the DNA damage response. J Cell Biol 2007;178:1101–8. [PubMed: 17893239]

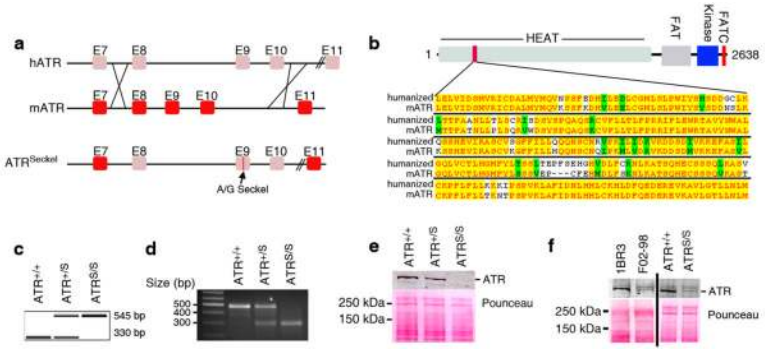

Figure 1. Generation of a humanized allele of the Seckel Syndrome

a, Schematic representation of the strategy to generate the mutant allele. The rearranged allele contains the genomic region encompassing human exons 8-10 (pink) inserted into the equivalent region of the murine *Atr* gene (red exons). The SS mutation is indicated in E9. **b,** Visualization of the location and sequence homology of the humanized ATR protein in the region encoded in E8-E10. The full-length quimeric protein presents a 99.1% homology with murine ATR. **c,** PCR genotyping, **d,** RT-PCR of ATR with primers at E8 and E10 and **e,** ATR western blot, of littermate MEF lines (**c-e**). **f,** ATR western blot in human fibroblast lines 1BR3 (control) and F02-98 (Seckel), together with $ATR^{+/+}$ and $ATR^{S/S}$ MEF.

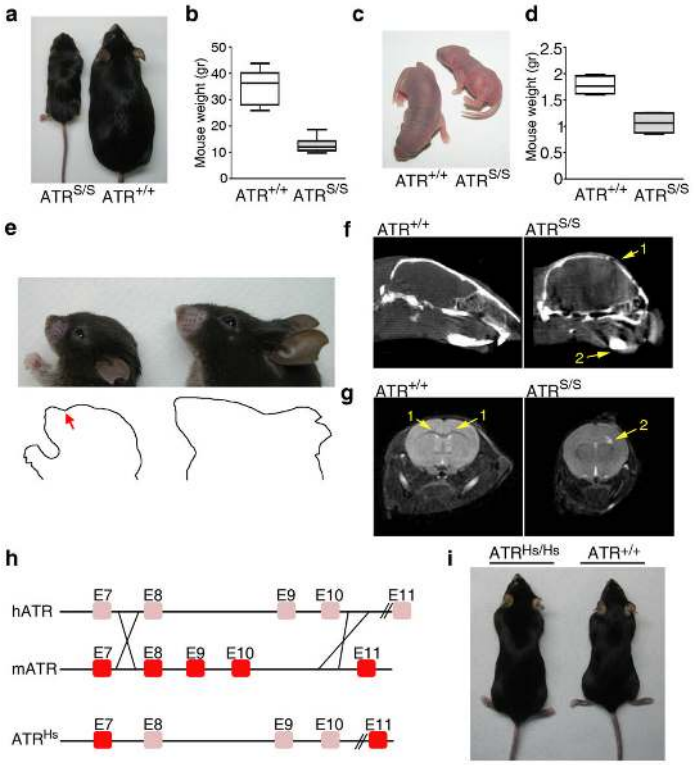

Figure 2. ATR$^{S/S}$ mice recapitulate the human SS

a, Representative pictures and weights of ATR$^{+/+}$ and ATR$^{S/S}$ mice at 3 months of age **a,b** or at birth **c,d**. **e,** Picture of the heads of ATR$^{+/+}$ and ATR$^{S/S}$ littermates. An outline is drawn to illustrate the protruding nose appearance (red arrow) due to the receding forehead. **f,** Computerized tomography (CT) of the heads of ATR$^{+/+}$ and ATR$^{S/S}$ littermates illustrating the receding forehead (1) and micrognathia (2). **g,** MRI scans illustrating the AgCC (1) and the presence of cysts (2) on Seckel brains. **h,** Schema of the control allele (ATR^{HS}) which is identical to ATR^{S} but lacks the SS mutation. **i,** Representative picture of a couple of 3 month-old ATR$^{+/+}$ and ATR$^{HS/HS}$ littermates.

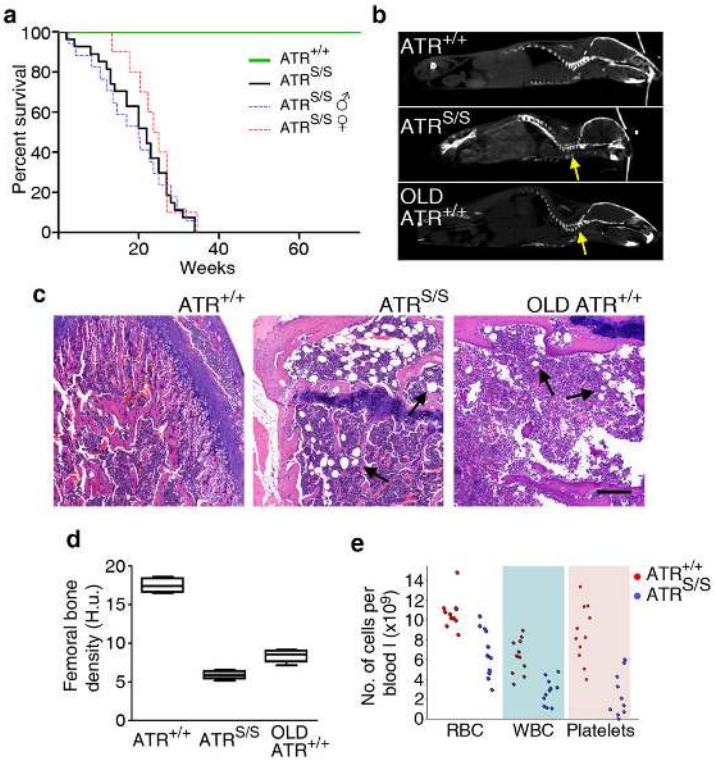

Figure 3. Premature ageing of ATR$^{S/S}$ mice

a, Kaplan-Meyer representation of the lifespan of ATR$^{+/+}$ (n=20) and ATR$^{S/S}$ (n=27) mice. **b,** CT of a pair of 2 month-old Seckel and control littermates, as well as an old (25 months) ATR$^{+/+}$ mouse. The yellow arrow indicates the presence of kyphosis. **c,** H/E staining from the femoral head of a pair of 2 month-old Seckel and control male littermates, as well as an old (25 months) ATR$^{+/+}$ male mouse to illustrate the accumulation of fat in the BM (black arrows). Scale bar indicates 200 μm. **d,** Distribution of the femoral bone density in ATR$^{+/+}$, ATR$^{S/S}$ and old (25-26 months) ATR$^{+/+}$ mice as a measure of the osteoporosis (n=7) (H.u.: Hounsfield unit). No significant gender differences were observed. **e,** Counts of platelets, red (RBC) and white (WBC) blood cells obtained from 3 month old ATR$^{+/+}$ and ATR$^{S/S}$ mice.

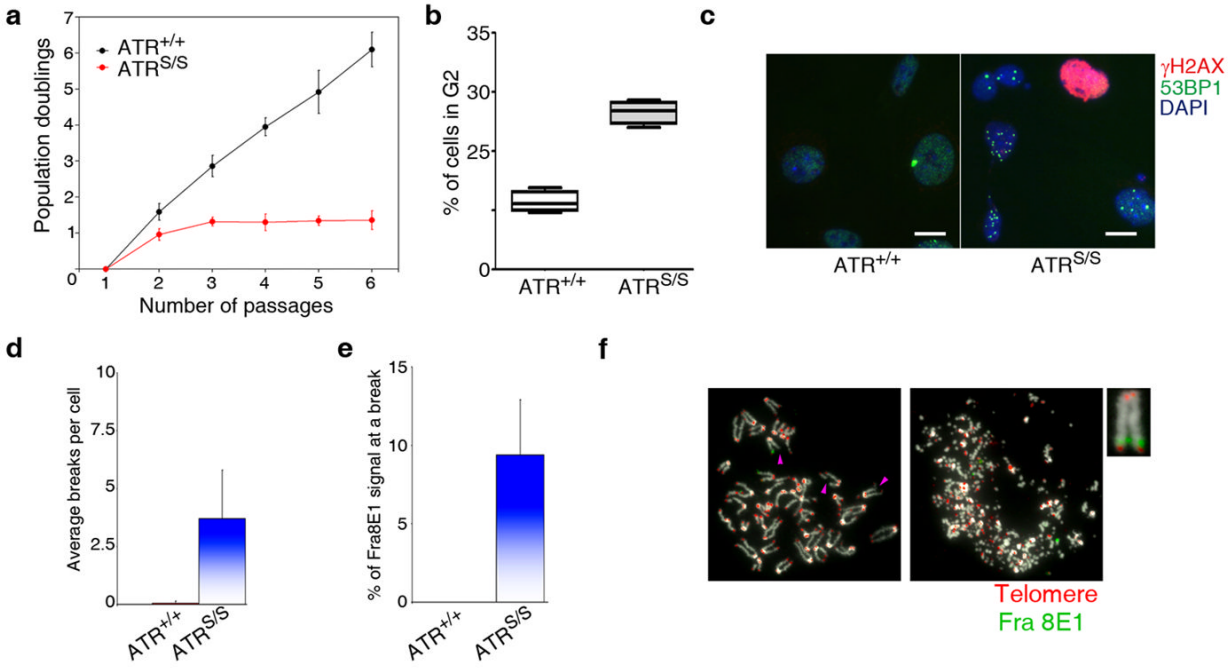

Figure 4. Accumulation of RS in ATR$^{S/S}$ MEF

a, Growth curves of ATR$^{+/+}$ and ATR$^{S/S}$ MEF. **b,** Percentages of cells at the G2 stage of the cell cycle derived from the analysis of DNA content by flow cytometry. **c,** Distribution of γH2AX and 53BP1 on ATR$^{+/+}$ and ATR$^{S/S}$ MEF. Scale bar indicates 5 μm. **d,** Average number of chromosome breaks per cell on control and Seckel metaphases. **f,** Percentage of the Fra8E1 alleles that were found to be at a break by FISH analyses. **e,** Representative images of the type of genomic aberrations found on ATR$^{S/S}$ MEF. Metaphases were stained with probes recognizing the telomeres and the Fra8E1 fragile site. 50 metaphases were analyzed per condition in 3 replicates.

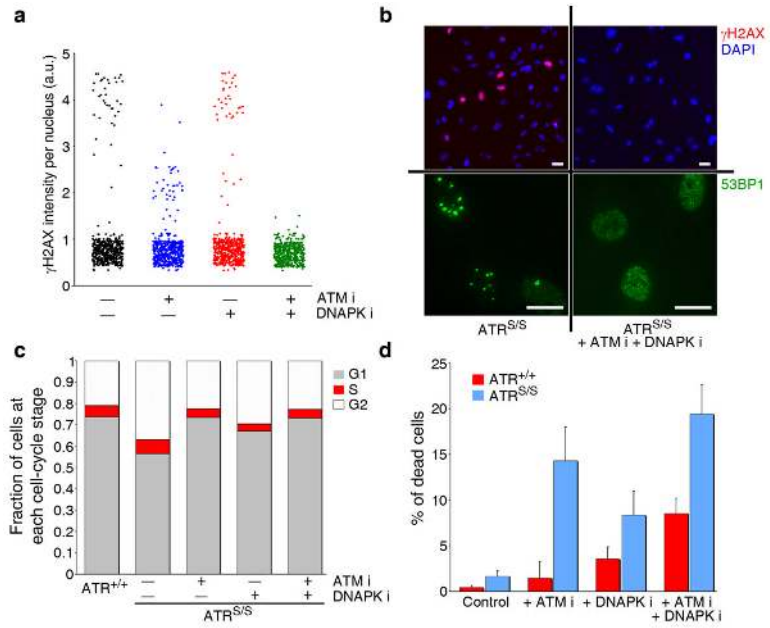

Figure 5. Response of ATR$^{S/S}$ MEF to PIKK inhibitors

a, High-Throughput microscopy data illustrating the distribution of γH2AX signal in wt and ATR$^{S/S}$ MEF treated with ATM and DNAPKcs inhibitors. **b,** Representative image from the analysis shown in **a** in the presence of both drugs. The distribution of 53BP1 is also shown below. **c,** Effect of the inhibitors on the G2 arrest observed on ATR$^{S/S}$ MEF. **d,** Percentage of dead cells found on ATR$^{+/+}$ and ATR$^{S/S}$ MEF cultures after 24 hrs of treatment with the inhibitors.

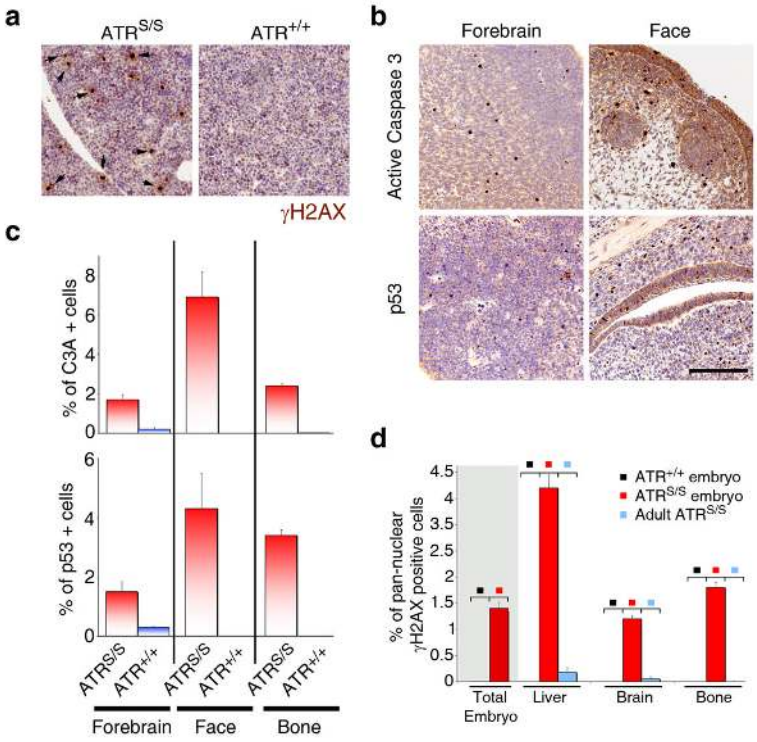

Figure 6. Accumulation of RS on ATR$^{S/S}$ embryos

a, Immunohistochemistry (IHC) of γH2AX on the liver of 13.5 dpc wt and Seckel littermate embryos. **b,** Examples of two representative areas of ATR$^{S/S}$ embryos, which were chosen from organs that appear compromised on adult mice -such as the forebrain or the face-, that illustrate the generalized accumulation of p53 or apoptotic cells (as measured with activated caspase 3) on the mutant embryos. Scale bar (white) indicates 150 μm. **c,** Quantification of the signals from **b**. **d,** Quantification of the frequency of cells with pan-nuclear γH2AX on different organs of 13.5dpc embryo and 2 month old mice.

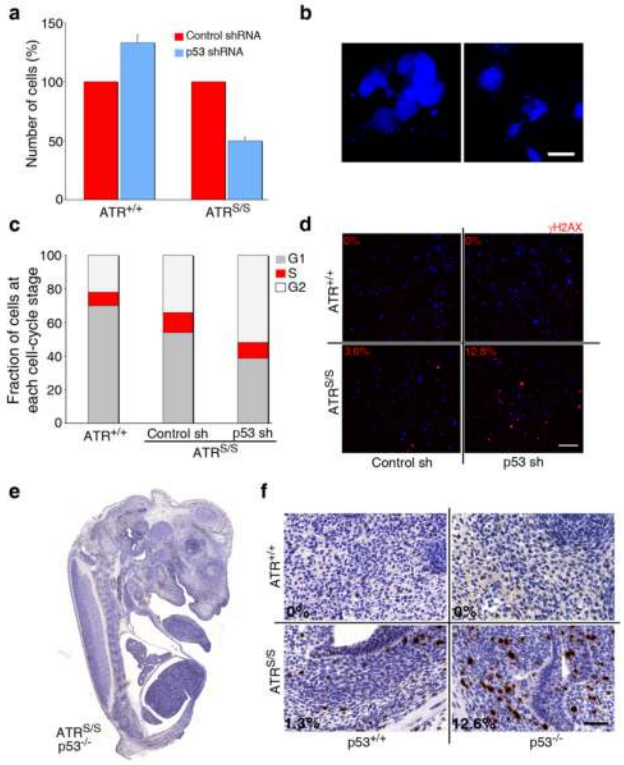

Figure 7. Effect of p53 depletion on ATR$^{S/S}$ cells and mice

a, Relative number of cells alive on ATR$^{+/+}$ and ATR$^{S/S}$ cultures after p53 depletion (see Methods). The number was normalized to cells infected with a control shRNA expressing lentivirus. **b,** Representative images of the type of abnormal nuclei found on p53 depleted Seckel MEF. Scale bar indicates 5 μm. Effect of p53 depletion on the G2 arrest (**c**) and γH2AX accumulation (**d**) observed on ATR$^{S/S}$ MEF. Scale bar indicates 100 μm. **e,** γH2AX IHC on a sagital section of a 13.5 dpc ATR$^{S/S}$/p53$^{-/-}$embryo. **f,** Magnification of a region close to the jaw on embryos from the different genotypes processed as in **e**. Scale bar indicates 50 μm.